Sink-source driven metabolic acclimation of winter oilseed rape leaves (Brassica napus L.) to drought

Mathieu Aubert, Vanessa Clouet, Florian Guilbaud, Solenne Berardocco, Nathalie Marnet, Alain Bouchereau, Younès Dellero

Journal of Plant Physiology 303 (2024) 154377

Contents lists available at ScienceDirect

Journal of Plant Physiology

journal homepage: www.elsevier.com/locate/jplph

Sink-source driven metabolic acclimation of winter oilseed rape leaves (Brassica napus L.) to drought

Mathieu Aubert [a], Vanessa Clouet [a], Florian Guilbaud [a], Solenne Berardocco [b], Nathalie Marnet [b], Alain Bouchereau [a,b,**], Younès Dellero [a,b,*]

[a] Institute for Genetics, Environment and Plant Protection (IGEPP), National Research Institute for Agriculture, Food and Environment (INRAE), Institut Agro Rennes-Angers, Université Rennes, France
[b] Metabolic Profiling and Metabolomic Platform (P2M2), MetaboHUB-Grand-Ouest, France

ARTICLE INFO

Keywords:
Amino acids
Gene expression
Metabolomics
Senescence
Starch
Tricarboxylic acid cycle

ABSTRACT

The crop cycle of winter oilseed rape (WOSR) incorporates source-to-sink remobilisation during the vegetative stage as a principal factor influencing the ultimate seed yield. These processes are supported by the coordinated activity of the plant's central metabolism. However, climate change-induced drought will affect the metabolic acclimation of WOSR sink/source relationships at this vegetative stage, with consequences that remain to be determined. In this study, we subjected WOSR to severe soil dehydration for 18 days and analysed the physiological and metabolic acclimation of sink and source leaves along the kinetics in combination with measurements of enzymatic activities and transcript levels. Overall, the acclimation of WOSR to drought led to subtle regulations of central metabolism in relation to leaf growth and Pro-induced osmotic adjustment. Notably, sink leaves drastically reduced their growth and transiently accumulated starch. Subsequent starch degradation correlated with the induction of beta-amylases, sucrose transporters, pyrroline-5-carboxylate synthases and proline accumulation. The functioning of the tricarboxylic acid cycle was also altered in sink leaves, as evidenced by variations in citrate, malate and associated enzymatic activities. The metabolic origin of Pro in sink leaves is discussed in relation to Pro accumulation in source leaves and the up-regulation of amino acid permease 1 and glutamine synthetase genes.

1. Introduction

Climate change is projected to increase the intensity and duration of heat waves and agricultural droughts in the next years (Pörtner et al., 2022; Zandalinas et al., 2021). In recent years, periods of agricultural drought have significantly affected plant growth, final seed yield elaboration and seed quality of the world's main crops, including maize, soybean, wheat and oilseed rape (Elferjani and Soolanayakanahally, 2018; Feller and Vaseva, 2014; Harkness et al., 2020; Sehgal et al., 2018; Wang et al., 2020). While some genetic strategies for developing climate change-resilient crops have emerged, there are still some unresolved questions regarding crop acclimation to drought (Verslues et al., 2023).

Winter oilseed rape (WOSR) is a major oleaginous crop in Europe with important applications in food and biofuels (Berrocoso et al., 2015). However, its crop cycle requires a substantial quantity of mineral nitrogen (N) in order to achieve maximal seed yield in comparison to other crops (Bouchet et al., 2016). WOSR has a low N remobilisation efficiency, resulting in the loss of 50% of the N initially absorbed (Malagoli et al., 2005). These losses are due to senescence-dependent leaf abscission, which occurs during the autumn vegetative stage and the spring/summer reproductive stage. Consequently, the management of source-to-sink nutrient remobilisation processes between leaves with

Abbreviations: BCAA, branched-chain amino acids; C, carbon; CS, citrate synthase; FC, field capacity; MDH, NAD-malate dehydrogenase; N, nitrogen; PEPc, phosphoenolpyruvate carboxylase; PPFD, photosynthetic photon flux density; RWC, relative water content; SMCSO, S-methyl-cysteine sulfoxide; SVWC, soil volumetric water content; TCA, tricarboxylic acid; WOSR, winter oilseed rape.

* Corresponding author. Institute for Genetics, Environment and Plant Protection (IGEPP), National Research Institute for Agriculture, Food and Environment (INRAE), Institut Agro Rennes-Angers, Université Rennes, France.
** Corresponding author. Metabolic Profiling and Metabolomic Platform (P2M2), MetaboHUB-Grand-Ouest, France.
E-mail addresses: mathieu.aubert@inrae.fr (M. Aubert), vanessa.clouet@inrae.fr (V. Clouet), florian.guilbaud@inrae.fr (F. Guilbaud), solenne.berardocco@univ-rennes.fr (S. Berardocco), nathalie.marnet@inrae.fr (N. Marnet), alain.bouchereau@univ-rennes.fr (A. Bouchereau), younes.dellero@inrae.fr (Y. Dellero).

https://doi.org/10.1016/j.jplph.2024.154377
Received 24 June 2024; Received in revised form 27 September 2024; Accepted 3 November 2024
Available online 6 November 2024

different phenological stages is determinant for the establishment of WOSR biomass and subsequently its seed yield (Avice and Etienne, 2014; Vazquez-Carrasquer et al., 2021). From a functional perspective, source-to-sink N remobilisation processes are supported by leaf senescence, which includes the dismantling of chloroplasts and the release of amino acids, sugars and lipids (Dominguez and Cejudo, 2021). Subsequently, these metabolites are transported to the phloem for source-to-sink export or directly degraded by catabolic pathways to fuel central metabolism and mitochondrial respiration (Barros et al., 2020; Chrobok et al., 2016). The maintenance of mitochondrial activity during senescence could sustain some energy-dependent remobilisation processes such as apoplasmic phloem loading (Nakamura and Izumi, 2018; Tegeder and Hammes, 2018). In WOSR, the phloem loading of amino acids represents a partial limitation to N remobilisation processes (Tilsner et al., 2005). Consequently, interactions between carbon (C) and N metabolisms in source leaves of WOSR are crucial for optimising nutrient remobilisation processes and plant growth (Dellero, 2020). Nevertheless, the metabolic functioning of sink leaves must also be considered. Despite exhibiting a high carbon utilisation rate in comparison to source leaves, their metabolic activity may be a limiting factor for the improvement of crop yield (Dethloff et al., 2017; Sonnewald and Fernie, 2018).

The process of plant acclimation to drought is mediated by the synthesis of abscisic acid in roots (sensing of soil drying), which is then transported through xylem vessels to leaf guard cells to reduce stomatal aperture and photosynthetic water losses (Kuromori et al., 2018; Tardieu et al., 2018; Urban et al., 2017). Hence, plants must contend with both water and carbon limitations during prolonged periods of drought, which has significant implications for source-to-sink relationships and the growth of WOSR (Batool et al., 2022). The resulting modulation of CO_2/O_2 ratios in the vicinity of the RuBiSCO will also impact C allocation to amino acids and the tricarboxylic acid (TCA) cycle (Dellero et al., 2021b; Fu et al., 2022). In WOSR, the quantity of N present in the soil is a significant determinant of metabolic acclimation to drought conditions (Albert et al., 2012, 2024). This emphasizes the central role played by amino acid metabolism during these processes. Indeed, prolonged periods of drought can simulate C starvation conditions, which in turn lead to the development of severe symptoms of senescence and the activation of branched-chain amino acid (BCAA) catabolism (Pires et al., 2016). The increased flux for TCA cycle intermediate biosynthesis during stress-induced senescence may result in a substantial change in its cyclic/non-cyclic flux modes in relation to stored organic acids such as citrate or malate (Dellero et al., 2023a; Destailleur et al., 2021; Le and Millar, 2022). In order to cope with the effects of stomatal closure, a metabolic reconfiguration can also operate to accumulate compatible osmolytes in *brassica* species such as sucrose or proline (Boulc'h et al., 2024; Slama et al., 2015). These osmolytes can contribute to the osmotic adjustment of leaf total water potential, but this process is accompanied by a metabolic cost (in terms of C and N elements, reducing power and energy) (Sanders and Arndt, 2012). In general, this osmotic adjustment is more pronounced in sink leaves of WOSR, primarily due to the accumulation of ions, sugars and amino acids (Boulc'h et al., 2024; Ma et al., 2004).

The overall acclimation of WOSR to drought appears to be closely associated with the regulation of source-to-sink remobilisation processes. Nevertheless, the metabolic functioning of sink and source leaves of WOSR in relation to drought-induced phenotypic adjustments remains to be addressed in the context of *brassica* crops (D'Oria et al., 2022; Fabregas and Fernie, 2019; Rosado-Souza et al., 2023; Xiong and Ma, 2022). The investigation of these processes could provide valuable insights for breeders interested in targeting source-to-sink remobilisation processes and sink strength for the improvement of oilseed rape resilience to drought. In this study, 9-week-old WOSR plants were subjected to soil dehydration for 18 days, with measurements and sampling conducted at 3–4 day intervals on sink and source leaves. The combination of physiological, biochemical and transcriptomic approaches enabled the identification of the early and late metabolic acclimation processes of WOSR sink and source leaves in relation to leaf growth and senescence. The results indicated an early accumulation of starch in sink leaves and suggested the involvement of multiple pathways in the biosynthesis of proline in sink leaves.

2. Material and methods

2.1. Plant growth and experimental design

The germination of *B. napus* L. genotype Aviso seeds (Bracycsol biological resource centre (IGEPP)) was initiated on soaked blotting paper for a period of 3 days after. Thereafter, the resulting seedlings were transferred to 4 L pots filled with a non-fertilised commercial substrate (Falienor reference 922016F3). The plants were cultivated in a greenhouse under the following conditions: 16 h light, 18–22 °C/8 h darkness, 15–19 °C. When necessary, sunlight was automatically supplemented with artificial lighting to maintain a minimum value of 150–200 µmol photons.$m^{-2}.s^{-1}$ (PPFD) at canopy height during the day. The plants were irrigated daily with a commercial fertilised solution (Liquoplant Bleu 2,5% N, 5% P, 2,5% K). Drought stress was applied to plants grown for 64 days after sowing. These plants possessed 12–13 leaf ranks at day 0, which were annotated from the bottom to the top (L1 to L13) (Fig. S1). The oldest leaf (L1) had fallen, indicating the initiation of source-to-sink remobilisation processes from old to young leaf ranks. Drought stress was conducted for 18 days by restricting irrigation to 40 mL per day (1 watering session) for the drought condition while the control condition was maintained at 600 mL per day (spread over 5 watering sessions). The volumetric water content of the soil (SVWC) was monitored throughout the experiment in six pots (3 controls, 3 drought conditions) using capacitive soil moisture probes (Yara ZIM). At different time points (0, 4, 8, 11, 15, 18 days), four individual plants per condition were selected and the leaves L4, L6 and L11 were used for different measurements (48 plants selected in total). The field capacity (FC, Fig. S1), representing the proportion of water retained within the soil, was determined based on the weight of the pots (comprising soil and container) measured at full hydration, then at each timepoint and finally after a complete soil dehydration (drying oven).

2.2. Physiological measurements, phenotyping and leaf sampling

The physiological measurements were taken in the morning while the phenotyping and leaf sampling occurred in the afternoon (8–10 h after the beginning of the light period, equivalent to midday). Chlorophyll contents were determined using the non-destructive chlorophyll SPAD-502 meter (Konica Minolta, Europe). Stomatal conductance (gs) was obtained from leaf gas exchanges measured with an LCi compact photosynthesis system (ADC BioScientific Ltd, Hertfordshire, UK) in a 6,25 cm^2 leaf chamber at ambient climatic conditions (20 °C, 150–200 PPFD, 430–450 µL $CO_2.L^{-1}$ air). The measurements were taken at least 3 h after the beginning of the light period, with the following constraints: a 2–3 min period of acclimation into the chamber and the use of a random order for processing plants and leaves. This random order allowed for the avoidance of potential time-dependent biases during measurements. For leaf phenotyping and sampling, each plant was processed individually (3 min per leaf). A randomly selected leaf (L4, L6 or L11) was cut at the petiole and the two limbs were excised with a blade in order to determine the leaf fresh weight (FW). Leaf area was subsequently measured with a LI-3100C Area Meter (LiCOR, Lincoln, NE, USA). Six leaf discs of 0.8 cm^2 were sampled on both limbs for relative water content (RWC) measurement. Each limb was then immediately frozen in liquid nitrogen. One limb was stored at −80 °C while the other limb was freeze-dried for approximately 100 h and ground into a fine powder to obtain the dry weight (DW) of the limb. Leaf DW was calculated as: leaf DW = (limb DW/limb area) *(total leaf area). Leaf expansion rate and leaf growth rate were calculated as the

slope of the linear regression between leaf DW and leaf area over time. For RWC measurements, leaf discs were weighed to determine the FW, then rehydrated for 2 h in the dark in ultrapure water to determine the turgid weight (TW). Finally, leaf discs were dried for 48 h in an oven at 70 °C to determine the DW. RWC was calculated according to the following equation: RWC (%) = ((FW-DW)*100)/(TW-DW).

2.3. Protein, starch, carbon and nitrogen contents

Soluble proteins were extracted from 10 mg of freeze-dried limbs in citrate-phosphate buffer and quantified using Bradford reagent and bovine serum albumin as a standard (Dellero et al., 2021a). The pellets resulting from these extractions were employed in the extraction of insoluble proteins using trichloroacetic acid and acetone (Wang et al., 2008). Starch was extracted from 10 mg of freeze-dried limbs and quantified in glucose equivalents using microplates (Gomez et al., 2007). The carbon (C) and nitrogen (N) contents were estimated using near infrared spectra and a custom predictive equation, which was constructed using 2000 samples of oilseed rape, following the procedures described in (Rolland et al., 2018).

2.4. Enzyme activities, ammonia and nitrate contents

Fresh limbs stored at −80 °C were grinded into a fine powder with a mortar and pestle in liquid nitrogen. Ammonia and nitrate were extracted and quantified using spectrophotometric assays following the formation of a nitrosalicylate ion or an ammonia-derived indophenol (Dellero et al., 2015). Enzymes were extracted from 120 to 150 mg of fresh limbs with 600 µL of a buffer containing 50 mM HEPES-KOH (pH 7.5), 10 mM $MgCl_2$, 1 mM EDTA, 1 mM EGTA, 10% glycerol, 0,1% Triton X-100, protease inhibitors (EDTA-free Protease Inhibitor Cocktail, Merck, Darmstadt Germany) and a small quantity of polyvinylpolypyrrolidone. The samples were briefly mixed and then kept at 4 °C for 5 min after which a centrifugation step of 5 min at 14 000 g and 4 °C was performed. The resulting supernatant (500 µL) was then desalted on a NAP-5 column (GE Healthcare) using 1 mL of 50 mM Hepes-KOH buffer (pH 7.5) for elution. Enzyme activities were quantified using a SpectraMax microplate reader (Molecular Devices) with 10–20 µL of the desalted samples. The activity of Sucrose synthase (SUSY) and neutral invertases (INV) was measured with an end-point assay by quantifying the amount of glucose produced by sucrose degradation (Biais et al., 2014; Turner et al., 2009). Acid INV activity was obtained by adding sorbitol to the extraction buffer in order to break the vacuoles. Citrate synthase (CS) activity was assessed by monitoring the consumption of acetyl-CoA using 5,5′-dithiobis-(2-nitrobenzoic acid) (Eigentler et al., 2020). Phosphoenolpyruvate carboxylase (PEPc) activity was quantified using a continuous assay methodology described by (Benard and Gibon, 2016). NAD-Malate dehydrogenase (NAD-MDH) activity was determined by monitoring the production of NAD at 340 nm in a reaction mixture containing 1 mM oxaloacetate, 500 mM Tricine-KOH (pH 8), 0.25% Triton X-100, 1 mM EDTA, 1.5 mM NADH (Gibon et al., 2004). All measurements were expressed per DW using the leaf FW/DW ratio to account for the dilution effect due to drought stress.

2.5. Quantitative analysis of transcript levels

Total RNA was extracted and subsequently processed in order to obtain cDNA in accordance with the methodology previously described (Dellero et al., 2020a). Quantitative PCR (qPCR) experiments were conducted using 4 µL of cDNA, which were diluted to 1/15, 5 µL of LightCycler 480 SYBR Green I Master mix (Roche) and 1 µL of primer pairs at 5 µM (Table S1). The qPCRs were performed on a Light Cycler LC480 (Roche) under the following conditions: an initial step at 95 °C for 5min, followed by 50 cycles of 95 °C for 15s, 60 °C for 15 s and 72 °C for 30s. Arabidopsis target genes were selected based on their potential role in senescence and drought (Have et al., 2017; Stein and Granot, 2019; Thalmann and Santelia, 2017). WOSR homologous genes were identified with a nucleotide BLAST search on the *B. napus* Darmor-bzh v10 reference genome (Rousseau-Gueutin et al., 2020). Subsequently, WOSR target genes were then selected based on the intensity of their leaf expression level, with the objective of ensuring an accurate detection by qPCR (logCPMs from a preliminary RNA-seq available in our team). qPCR primers were designed to amplify a single gene when possible (qPCR product at 100–300 bp). The suitability of primers was validated using melting curves and by calculating the primer efficiency from a serial dilution of mixed samples from our experiment. The three reference genes *RibS3*, *UBQ11* and *SBP1* were selected for their expression stability (Fig. S2) using the GeNorm method (Hellemans et al., 2007). Gene expression was calculated by considering the efficiency of each qPCR primer pair, the conversion of Cq values into relative quantities and the sample-specific normalisation factor (reference genes), as described in (Hellemans et al., 2007). For each gene, relative expression levels were normalised to the "Control_leaf11_day8" samples, with the mean value set to 1.

2.6. Quantitative analysis of polar metabolites by GC-FID and UPLC-DAD

Polar metabolites were extracted from 10 mg of freeze-dried limbs in a methanol/chloroform/water buffer containing 200 µM of DL-3-aminobutyric acid (BABA) and 400 µM of adonitol as internal standards following procedures described in (Dellero et al., 2020b). A total of 50 µL of the upper polar phase (MeOH/H_2O fraction) was used for each analysis. Amino acids were derivatised using the AccQTag derivatisation kit (Waters) and analysed by UPLC-DAD in accordance with the procedures described in (Renault et al., 2010). Sugars, polyols and organic acids were derivatised using methoxyamine and MSTFA and analysed on a Trace 1300 GC-FID according to procedures described in (Bianchetti et al., 2021). Peak identification and absolute quantification were achieved using retention times and known concentrations of the derivatised authentic standards. Peak integration was performed using the manufacturer's software, and the results were manually inspected and corrected as necessary. Additionally, "quality control" (QC) samples were created by randomly selecting samples and combining them to assess inter-run variations and normalise all the values acquired (Fig. S3). The concentration of compounds was quantified in µmol. g^{-1}DW by normalising raw areas to the following: i) the internal standards (BABA for amino acids; Adonitol for sugars, polyols and organic acids), ii) the external calibration curves of standards, iii) the DW of the samples and iv) the inter-run variations of QC samples.

2.7. Statistical analysis

Data were treated and visualised using tidyr, dplyr, ggplot2, ComplexHeatmap, car and multcompletters packages from Rstudio (2022.07.2 + 576) (RStudio Team, 2022). Sparse Partial Least Square Discriminant Analysis (sPLS-DA) was conducted using the MixOmics package on metabolites detected in at least 80% of the samples. Missing value imputation was performed using the half-minimum method (Wei et al., 2018). Heatmap representations were generated using log2 fold-change values, without centring and scaling the data. Statistical analyses of fold-changes for metabolites were performed on untransformed data. Prior to the application of statistical tests on qPCR fold-changes, each value for each sample was log-transformed. A multifactor analysis was conducted using a three-way ANOVA (type III; p-value$<$0.05). Post-hoc comparison of multiple groups of means was achieved with a Tukey HSD test while statistical comparison of two groups of means was achieved with a Student test (p-value$<$0.05). All data represent the mean ± standard deviation (SD) for 3–4 independent biological replicates.

3. Results

3.1. Drought exerts differential impacts on the growth, water content and biomass composition of WOSR sink and source leaves

Following the imposition of water restrictions on 64-day-old WOSR plants, the soil volumetric water content decreased rapidly during the first 8 days of drought and reached a plateau at 3–5% from day 8 to day 18, equivalent to a field capacity of 10–20% (Fig. 1A, Fig. S1). Two types of acclimation responses were identified: early responses (days 4–8) and late responses (days 11–18). Control plants possessed eleven leaf ranks at day 0, with the oldest leaf at the bottom (leaf 2) and the youngest leaf at the top (leaf 12). Drought only marginally impacted leaf ontogenesis (Fig. S1). For subsequent analyses, three leaf ranks were selected, namely 11, 6, and 4. Leaf 11 was a sink leaf, as reflected by its important leaf growth (biomass, area) and higher stomatal aperture compared to other leaves in the control condition (Fig. 1, Figs. S1 and S4). Leaf 4 was identified as a source leaf, characterised by the absence of growth, low stomatal aperture and low leaf biomass/leaf area. Leaf 6 was classified as a mature leaf, exhibiting morphological and physiological characteristics intermediate between those of a source and a sink leaf. After 4–8 days of water restrictions, all leaves exhibited statistically significant reductions in stomatal conductance to water vapor and relative water content (RWC) (Fig. 1, Table S4). Drought also stopped growth for the sink leaf (biomass, area) starting from day 8 and accelerated leaf abscission of old leaves, with the leaf 3 being dropped after day 11 versus day 15 for the control condition (Fig. 1, Fig. S1, Table S4). The expression of some drought-responsive genes was also induced at day 8

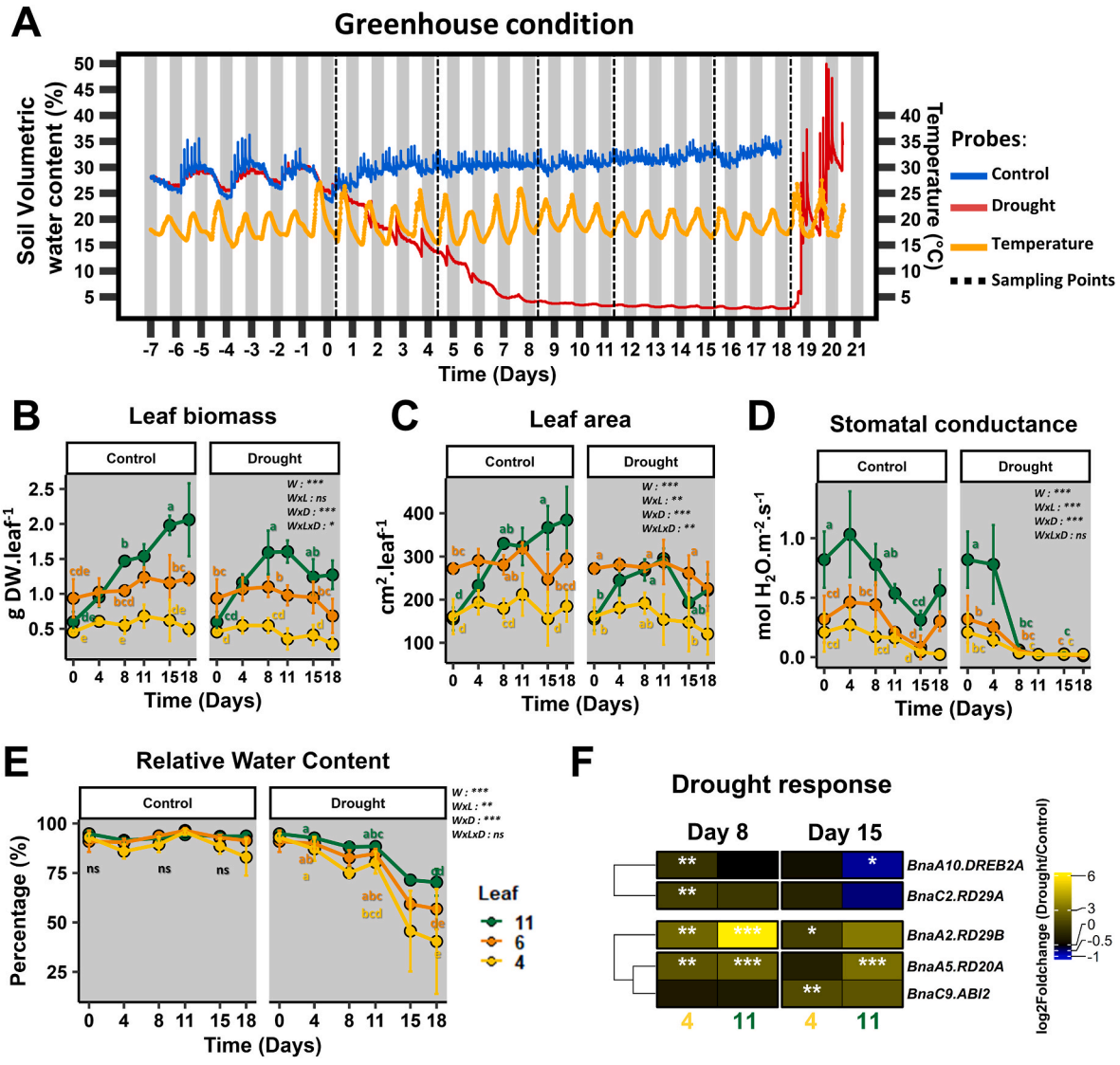

Fig. 1. Morphological and physiological responses of sink and source leaves of oilseed rape under drought stress. (**A**) Soil humidity and temperature, (**B**) leaf area, (**C**) leaf biomass, (**D**) stomatal conductance, (**E**) relative water content and (**F**) relative expression of drought-responsive genes through abscisic acid-dependent (*RD29B, RD20A, ABI2*) and -independent pathways (*DREB2A, RD29A*). Drought stress was applied for 18 days and followed by 2 days of rehydration. Leaf ranks were annotated from the bottom to the top of the plant according to their date of appearance (3–11). qPCRs were performed with the primers listed in Table S1 using three different reference genes that showed robust expression stability across samples (Fig. S2). Normalised transcript levels were expressed relative to leaf 11 of control plants at day 8. All data represent the mean ± SD of 3–4 biological replicates. The effect of the factor "water" (*W*) in combination with the factors "leaf" (*L*) and "day" (*D*) was evaluated with a three-way ANOVA (ns, not significant; *, p-value<0.05; **, p-value<0.01; ***, p-value<0.001). Post-hoc analyses were performed on separate conditions (control or drought) at days 0, 8 and 15 using the Tukey HSD test (p-value<0.05; statistical groups indicated with different letters). For qPCRs, normalised values were log-transformed before applying a *t*-test for each fold-change (*, p-value<0.05; **, p-value<0.01; ***, p-value<0.001). The complete datasets are available in Fig. S5 and Tables S2 and S4.

and day 15 in both sink and source leaves, but essentially for abscisic acid-dependent pathways (*RD29B*, *RD20A*) (Fig. 1F). Interestingly, a clear gradient of RWC was observed between the leaves, starting after day 8 and becoming more pronounced over time. This suggested that the metabolic acclimations of the sink and source leaves were different. The analysis of senescence markers (chlorophyll, proteins, %C, %N, *Cab1/Sag12* balance) in the control condition confirmed the sink and source status of the selected leaves (sink with high levels, source with low levels) (Fig. 2). A significant decline in chlorophyll content was observed in the leaf 4 and 6 during the drought period, while the leaf 11 showed minimal effects (Fig. 2A–Table S4). A specific analysis of protein contents in the leaves 11 and 4 revealed a substantial decline of both soluble and insoluble proteins after 8 and 15 days of drought (Fig. 2B). C content followed the same trend as for chlorophyll content, while N content was significantly reduced in the leaves 11 and 6 along the kinetics (Fig. 2C and D, Table S4). Furthermore, drought induced a reduction in *Cab1* expression in leaf 11 at days 8 and 15, while *SAG12* expression, encoding a senescence-associated cysteine protease, was increased in leaf 4 (Fig. 2E). *SAG12* expression in leaf 4 was significantly elevated between days 8 and 15, thereby confirming a significant induction of senescence in source leaves following long-term water restriction. In conclusion, the early responses of WOSR leaves to drought (days 4–8) were characterised by a rapid decrease in stomatal conductance and low protein, total leaf N, RWC and growth levels in all leaves. In contrast, the late responses of WOSR leaves to drought (days 11–18) exhibited differential patterns between sink and source leaves. The sink leaf 11 demonstrated the maintenance of chlorophyll levels and RWC while the source leaf 4 exhibited a more severe response, characterised by intensive dehydration and accelerated senescence. This was evidenced by a combination of chlorophyll and protein degradation, accompanied by an increase in *SAG12* expression.

3.2. *Drought induces metabolic reconfiguration in WOSR sink and source leaves*

Targeted quantification of sugars, polyols, organic and amino acids was conducted for all leaves and at each timepoint. A global discriminant analysis (SPLS-DA) enabled the differentiation between control and drought conditions for the sink leaf (leaf 11) and the source leaf (leaf 4) (Fig. 3A). The predictive component 1 (x-variate 1), which was constructed to maximise the separation of control and drought conditions, explained 44% of the total variance within the metabolic dataset. Conversely, the component 2 (x-variate 2), which was constructed to maximise intra-group separation, only explained 10–17% of the total variance and partially reflected timepoint separation. For the sink leaf 11, correlation circle plots identified significant contributions to

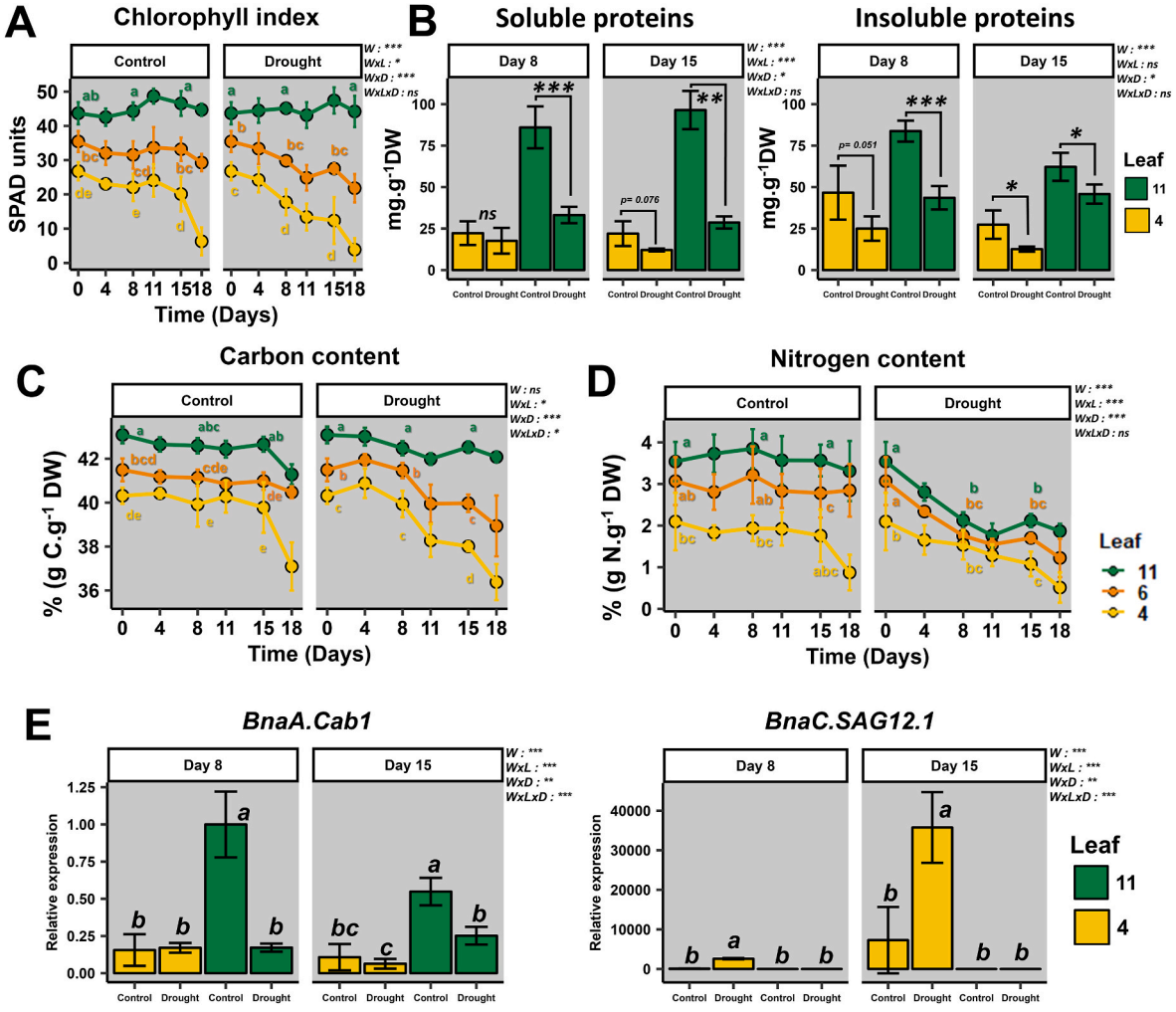

Fig. 2. Senescence markers in sink and source leaves of drought-stressed oilseed rape. (**A**) Chlorophyll content, (**B**) soluble and insoluble protein content, (**C**) carbon content, (**D**) nitrogen content and (**E**) relative expression levels of *Cab1* and *SAG12.1* genes. qPCRs were performed and analysed exactly as described in Fig. 1. All data represent the mean ± SD of 3–4 biological replicates. Statistical tests were applied exactly as described in Fig. 1 (three-way ANOVA followed by post-hoc Tukey HSD test on either "control" or "drought" conditions). For protein contents, a *t*-test was performed for each leaf on each day by comparing control and drought conditions (*, p-value<0.05). The complete datasets are available in Tables S2 and S4.

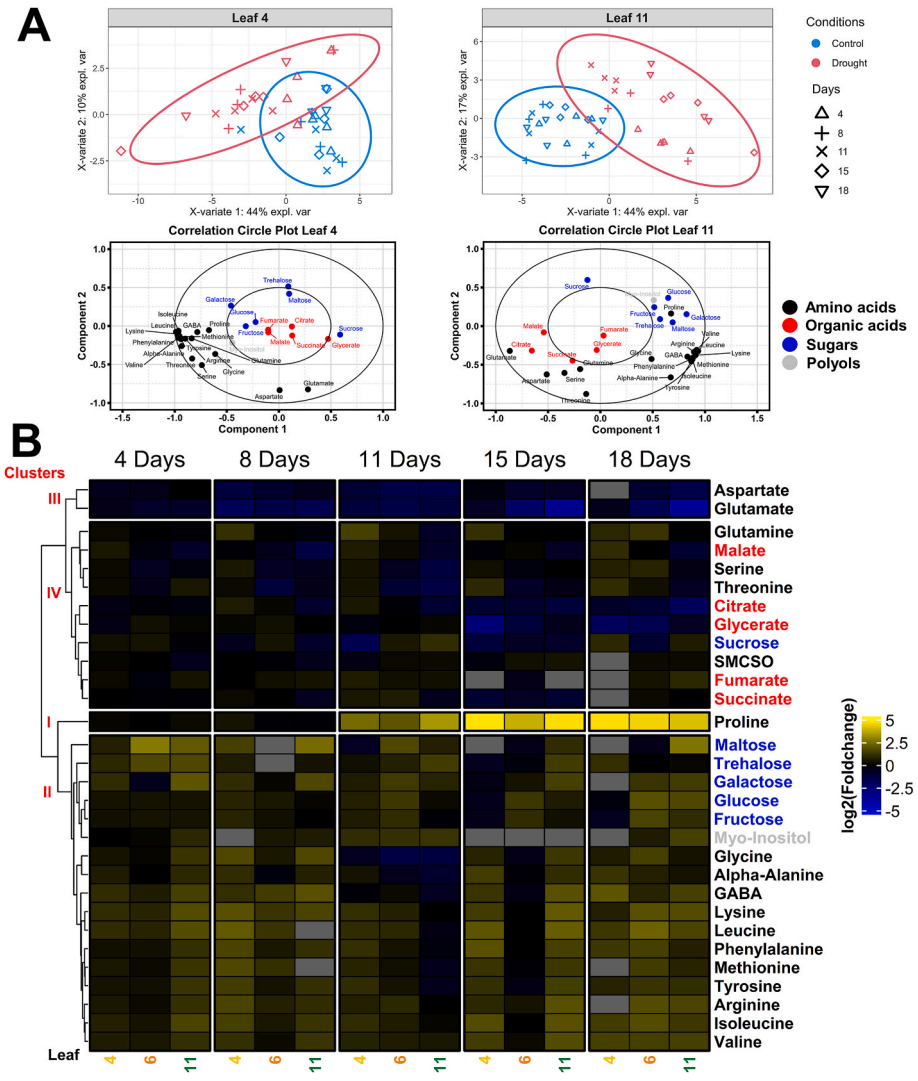

Fig. 3. Identification of metabolic signatures associated with sink/source status and acclimation to drought. (**A**) Sparse Partial Least-Square Discriminant Analysis (sPLS-DA) for the leaves 11 and 4 (score plot and correlation circle plot), (**B**) heatmap of log2 fold-changes in metabolite content between drought and control conditions in sink and source leaves of oilseed rape during 18 days of drought. Metabolites (sugars, polyols, organic and amino acids) were quantified using UPLC-UV and GC-FID with external calibration curves and were normalised to the internal standards, quality control samples and dry weight (3–4 biological replicates). Metabolites not detected in the samples (less than 3 biological values) are shown in grey boxes. Hierarchical clustering analysis of log2 fold-changes was based on the Euclidean distance matrix. The sPLS-DA was performed without timepoint 0 because there was only one growth condition (control). sPLS-DA ellipses represent 95% confidence intervals for the separation of control (blue) and drought (red) conditions. The complete datasets are available in Tables S2 and S4. (For interpretation of the references to colour in this figure legend, the reader is referred to the Web version of this article.)

predictive component 1 for numerous amino acids (Pro, Glu, Gln, Asp, Ala, Val, Phe, Leu, Ile; black points), some sugars (blue points) and organic acids such as citrate, malate and succinate (red points). Indeed, Pearson correlation coefficients ranged between 0.5 and 1 (the two black circles) for these metabolites. Conversely, the separation of control and drought conditions in the source leaf 4 was largely attributed to the influence of all amino acids (black points) and sucrose (blue points). A detailed analysis of the fold-change variations between drought and control conditions for all leaves revealed the presence of four distinct metabolic clusters (Fig. 3B). Pro constituted a separate group (cluster I) and exhibited a pronounced accumulation in all leaves following 8–18 days of drought. Some minor amino acids (BCAA, aromatic amino acids, Lys, Arg, Met) and major sugars also followed a similar trend in cluster II, albeit with a narrower range. Overall, compounds in cluster II showed a moderate accumulation in sink leaf 11 relative to other leaves, with the exception of day 11. Cluster III comprised only Glu and Asp, which levels were significantly reduced during drought, with a greater decrease observed in leaf 11. Cluster IV comprised sucrose, TCA cycle organic acids (succinate, fumarate, malate, citrate) and some major amino acids in WOSR: S-methyl-cysteine sulfoxide (SMCSO), Gln, Ser. Metabolites in this cluster showed a delayed response and exhibited contrasting variations between the leaves 4 and 11. Interestingly, Gln levels increased substantially in the source leaf 4 compared to the sink leaf 11, and may be indicative of the activation of source-to-sink remobilisation processes. To further elucidate the sink/source-driven metabolic acclimation of WOSR leaves to drought, we combined detailed analyses of some metabolite contents in the leaves 11 and 4 with measurements of enzymatic activities and transcript levels for key steps in starch/sugar metabolism, the TCA cycle, Pro biosynthesis and N remobilisation.

3.3. The regulation of starch and sucrose metabolism in WOSR sink and source leaves during drought

The soluble sugars (glucose, fructose) exhibited weak variations in both sink and source leaves under control conditions (Fig. 4A). However, a significant increase was observed in the sink leaf compared to the

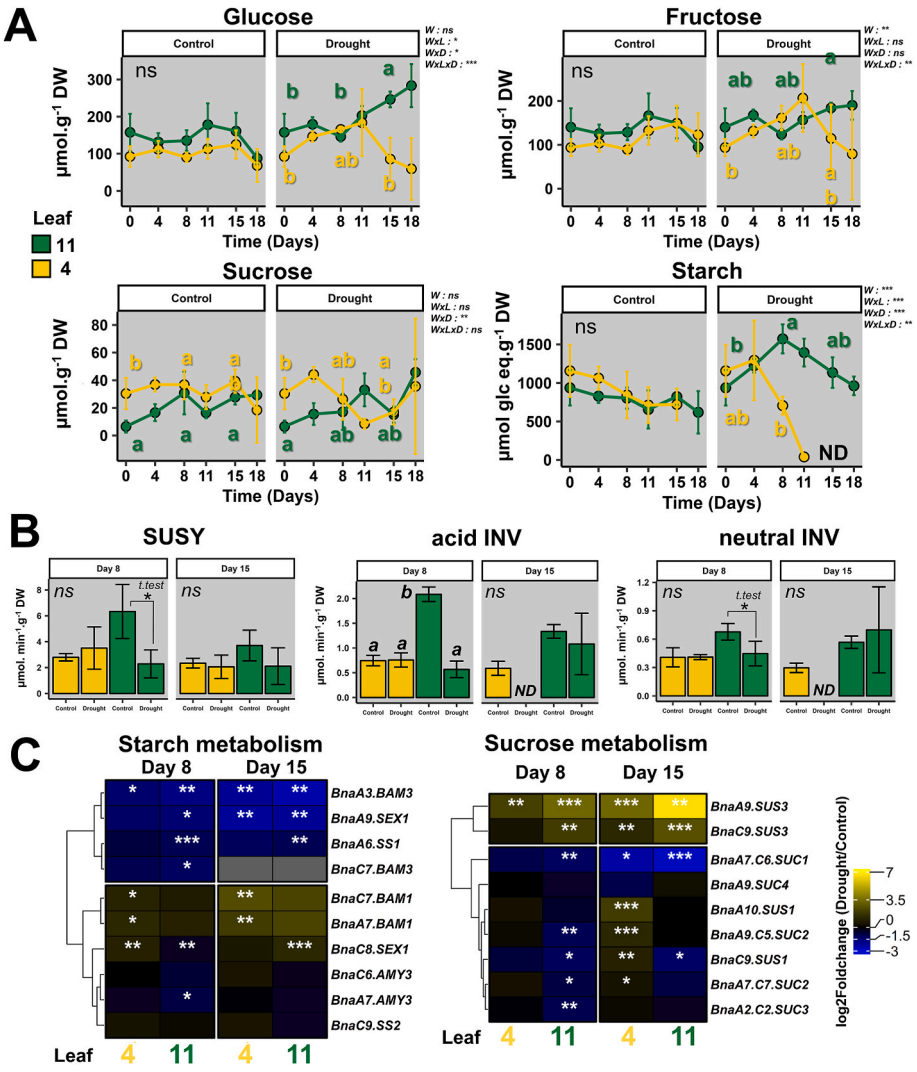

Fig. 4. Regulation of sucrose and starch metabolism during drought in sink and source leaves of oilseed rape. (**A**) Glucose, fructose, sucrose and starch levels in the leaves 11 and 4, (**B**) Total leaf enzyme activities for sucrose synthase (SUSY) and acid and neutral invertases (INV) in the leaves 11 and 4, (**C**) heatmap of log2 fold-change expression levels (qPCR) for key genes involved in the regulation of sucrose and starch metabolism after 8 and 15 days of drought in leaves 11 and 4. Starch was quantified at midday of the photoperiod and expressed as glucose equivalent (Glc eq). qPCRs were performed and analysed exactly as described in Fig. 1. When the primers amplified the two orthologous copies of a gene (subgenomes A and C; *SUC1* genes), the gene name was written as "BnaA.C". All data represent the mean ± SD of 3–4 biological replicates. Statistical tests for metabolite levels and qPCRs were performed exactly as described in Fig. 1. For enzyme activities, statistical differences between samples at days 8 and 15 were assessed separately using one-way ANOVA followed by post-hoc Tukey HSD test (p-value<0.05). If the post-hoc test did not identify different groups, a *t*-test was performed for each leaf on each day by comparing control and drought conditions (*, p-value<0.05). ND, not detected. The complete datasets are available in Figs. S6 and 7 and Tables S2–4.

source leaf after 15–18 days of drought. Conversely, sucrose levels were larger in the source leaf at the beginning of the experiment, but showed weak variations during drought (due to large biological variability). Quite surprisingly, starch levels at midday were significantly larger in the leaf 11 at day 8, and only returned to basal levels at day 15. In the source leaf 4, starch levels were significantly decreased along the kinetics, reaching undetectable amounts at day 15–18. The regulation of metabolic acclimation was then investigated with measurements of enzyme activities and gene expression for the leaves 11 and 4 on days 8 and 15. The activity of sucrose synthase (SUSY) and acid and neutral invertases (INV) was significantly decreased during drought, although this was only observed on day 8 and for leaf 11. However, the decrease observed for neutral INV was relatively low, suggesting that this activity was still maintained in the leaf 11 during drought. Interestingly, *BAM1* genes were significantly up-regulated by drought in source leaf tissues (Fig. 4C, Fig. S6), and they might significantly contribute to drought-induced starch degradation. Indeed, other genes that play similar roles during drought or cold stress in Arabidopsis such as *AMY3* or *BAM3*, had an opposite trend and did not correlate with starch degradation in source leaves (Fig. 4). Regarding starch biosynthesis, *SS1* was down-regulated by drought while the expression of *SS2* remained relatively stable (Fig. 4C, Fig. S6). Although *SEX1* genes exhibited contrasting expressions during drought, the overall regulation of starch synthesis was relatively negative during drought in both sink and source leaves. The regulation of sucrose metabolism was then evaluated by considering sucrose synthase (SUS) and sucrose transporters (SUC). Overall, *SUS3* genes were significantly up-regulated by drought in sink and source leaves while *SUS1* genes showed opposite patterns (Fig. 4C). However, *SUS1* genes were significantly up-regulated in the source leaf 4 at day 15. The *SUC3* and *SUC4* genes were not significantly regulated in response to drought while *SUC1* expression was significantly reduced in both sink and source leaves. Interestingly, *SUC2* genes were significantly up-regulated in sources leaves but were also significantly down-regulated in sink leaves. This may suggest the activation of source-to-

sink remobilisation of sucrose during drought. Nevertheless, the transcriptional regulation of sucrose and starch metabolism by drought only partially correlated with the evolution of starch and sucrose contents in sink and source leaves.

3.4. The impact of drought on TCA cycle organic acids and some associated enzyme activities

Malate and citrate were the most abundant TCA cycle organic acids detected in sink and source leaves (30–40 μmol g^{-1} DW) in comparison to fumarate and succinate (1–2 μmol g^{-1} DW) (Fig. 5A). These observations suggested a potential role for malate and citrate in C storage in WOSR leaves. During drought, the citrate content of the sink leaf had significantly decreased in comparison to the source leaf (from 30 to 10 μmol g^{-1} DW). Drought also significantly restricted the accumulation of malate in the sink leaf during the kinetic phase (Table S4). Conversely, citrate and malate levels remained stable in the source leaf 4. When comparing day 0 and day 18 during drought, fumarate content increased in the sink leaf 11 while succinate content decreased. These results were likely indicative of modifications to the metabolic fluxes of the TCA cycle in the sink leaf. Subsequently, the regulation of TCA cycle was investigated through the measurement of total leaf enzyme activities for citrate synthase (CS), NAD-malate dehydrogenase (NAD-MDH) and phosphoenolpyruvate carboxylase (PEPc), given that the TCA cycle is preferentially regulated by post-translational modifications (da Fonseca-Pereira et al., 2021; Nunes-Nesi et al., 2013). Drought significantly reduced CS activity in sink leaves and correlated with a reduction in citrate content (Fig. 5B). However, both PEPc and NAD-MDH activities were also partially reduced in sink and source leaves during drought and only partially correlated with the evolution of malate content. In conclusion, drought appears to reduce TCA cycle activity in both leaves, thereby challenging the metabolic origin of Pro in sink leaves (TCA cycle *de novo* biosynthesis or use of stored molecules (citrate, proteins)).

3.5. Pro biosynthesis and N remobilisation during drought in sink and source leaves

In response to drought, both sink and source leaves showed a significant accumulation of Pro after 11 days (Fig. 6A, Table S4). However, leaf 11 showed a higher accumulation of Pro compared to leaf 4. This capacity to accumulate Pro was strongly correlated to the RWC and the regulation of *Proline-5-carboxylate synthase 1* (*P5CS1*) genes in terms of intensity and statistical significance (Figs. 1E and 6B). Consequently, Glu utilisation for Pro biosynthesis in source leaves may have affected source-to-sink remobilisation of N. The contents of Glu and Gln were

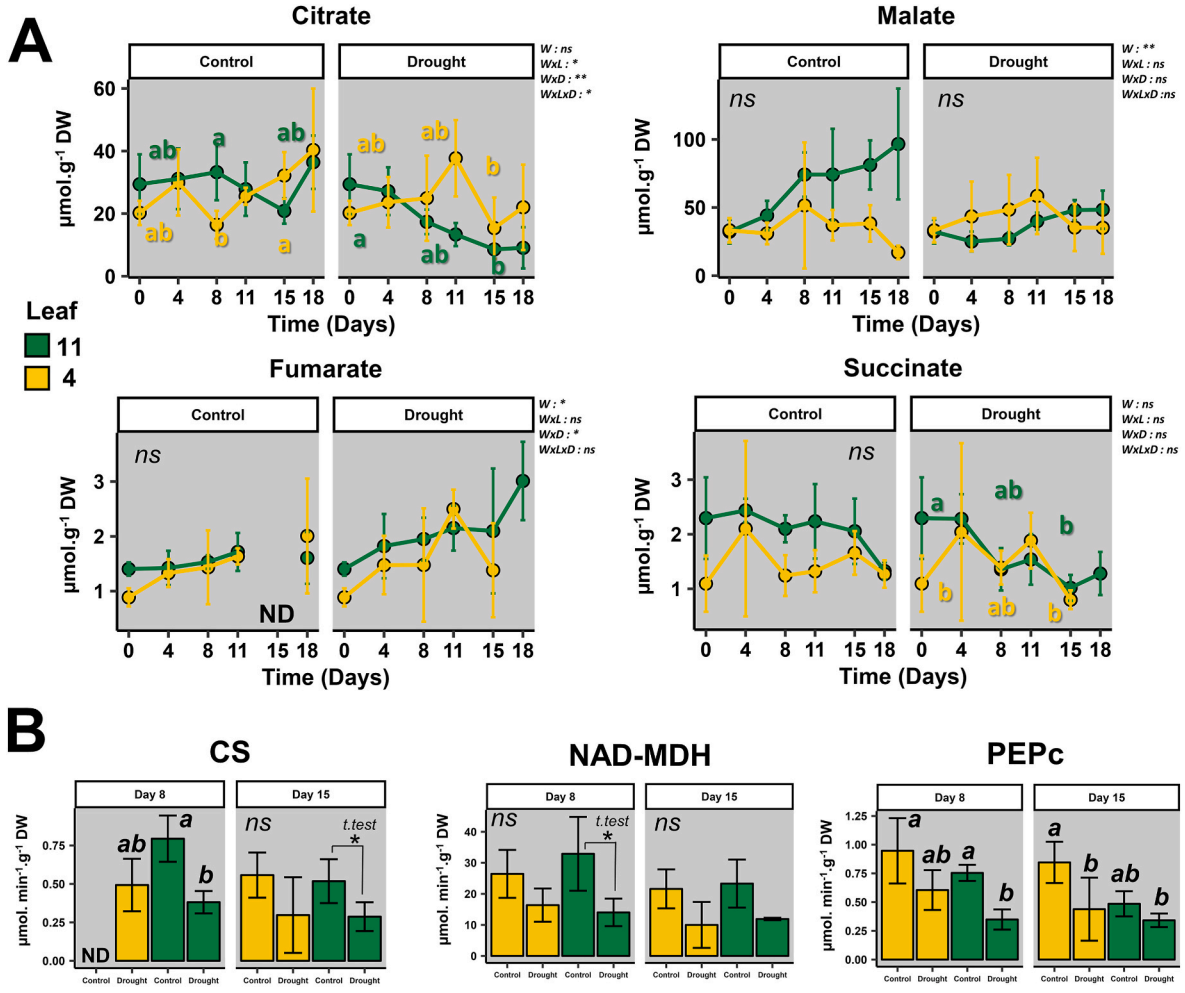

Fig. 5. Levels of TCA cycle organic acids and associated enzyme activities during drought in sink and source leaves of oilseed rape. (**A**) Citrate, malate, fumarate and succinate contents in leaves 11 and 4, (**B**) Total leaf enzyme activities for citrate synthase (CS), malate dehydrogenase (NAD-MDH) and phosphoenolpyruvate carboxylase (PEPc) in the leaves 11 and 4. All data are mean ± SD of 3–4 biological replicates. ND, not detected. For metabolite contents, statistical tests were performed exactly as described in Fig. 1. For enzyme activities, statistical differences between samples at days 8 and 15 were assessed separately using one-way ANOVA followed by post-hoc Tukey HSD test (p-value<0.05). If the post-hoc test did not identify different groups, a *t*-test was performed for each leaf on each day by comparing control and drought conditions (*, p-value<0.05). ND, not detected. The complete datasets are available in Tables S2–4.

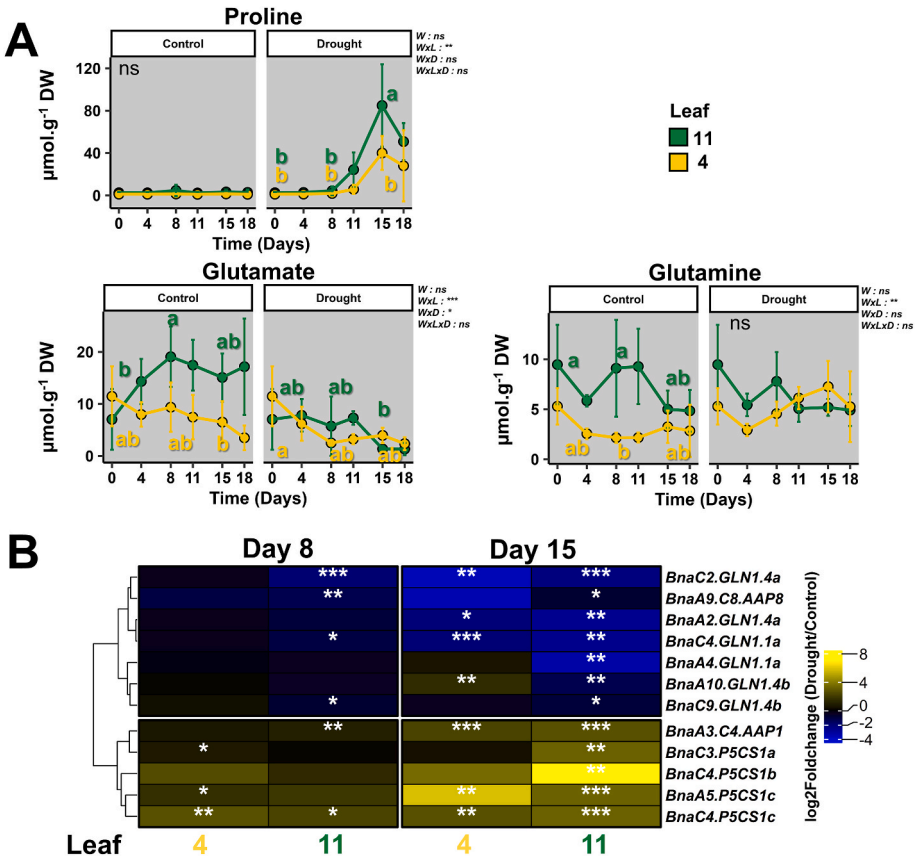

Fig. 6. Regulation of proline biosynthesis and amino acid remobilisation during drought in sink and source leaves of oilseed rape. (**A**) Proline, glutamate and glutamine levels in leaves 11 and 4, (**B**) heatmap of log2 fold-change expression levels (qPCRs) for key genes involved in the regulation of proline biosynthesis and amino acid remobilisation after 8 and 15 days of drought in leaves 11 and 4. qPCRs were performed and analysed exactly as described in Fig. 1. When the primers amplified the two orthologous copies of a gene (subgenomes A and C; *AAP1* and *AAP8* genes), the gene name was written as "BnaA.C". All data represent the mean ± SD of 3–4 biological replicates. Statistical tests for metabolite levels and qPCRs were performed exactly as described in Fig. 1. The complete datasets are available in Figs. S8 and 9 and Tables S2–4.

found to be higher in leaf 11 than in leaf 4. However, drought induced minor modifications in leaf 4 (Fig. 6A). Only the Glu content decreased in leaf 11 during drought, perhaps reflecting its commitment towards Pro biosynthesis. Subsequently, the regulation of N remobilisation was evaluated through gene expression analysis of specific amino acid transporters (*AAP1 and AAP8*) and glutamine synthetases (*GLN1.1 and GLN1.4*) that are involved in these processes. Here, *AAP1* genes rather than *AAP8* genes were significantly up-regulated by drought in the leaves 11 and 4 (Fig. 6B). Indeed, *AAP8* was mostly expressed in sink leaf and was down-regulated during drought (Fig. S9). Therefore, *AAP1* may be involved in phloem loading and unloading of amino acids during drought in WOSR. The *GLN1.1* and *GLN1.4* genes were monitored and found to be almost all down-regulated during drought in leaf 11. This could reflect a decrease in *de novo* N assimilation in relation to the decrease in Glu content. Regarding the source leaf 4, some important contrasts were observed. While the majority of *GLN1.1* genes exhibited a pronounced downregulation, *BnaA.GLN1.1a* and *BnaA.GLN1.4b* genes demonstrated a slight upregulation at day 15 (Fig. 6B). Notably, these genes exhibited higher expression levels in leaf 4 relative to leaf 11, a pattern similar to that observed for *AAP1* (Fig. S9). Consequently, source-to-sink remobilisation of N may have been partially maintained during drought, with the potential to contribute to *de novo* Pro biosynthesis in sink leaves. The level of other amino acids previously identified in the heatmap was also analysed (Fig. 3, Fig. S10). However, they showed a significant biological variability, with the exception of Asp, which followed a similar pattern to that observed for Glu.

4. Discussion

The crop cycle of WOSR is markedly influenced by source-to-sink remobilisation processes but the acclimation to drought could have a substantial impact on these processes. Hence, the investigation of sink-source driven metabolic acclimation of WOSR to drought is a prerequisite for the development of targeted genetic strategies for the improvement of WOSR resilience to drought. In this study, a multidisciplinary approach was employed to identify contrasting acclimation strategies between sink and source leaves.

4.1. *Transient accumulation of starch as an early metabolic indicator of drought in sink leaves*

The activation of starch degradation during drought has been observed in numerous plant species, allowing for the provision of energy and carbon at times when photosynthesis is necessarily limited (Park et al., 2021; Thalmann and Santelia, 2017; Zanella et al., 2016). A comparable pattern was observed in the source leaf during the period of drought perception (days 4–8), which was accompanied by the up-regulation of beta-amylase *BAM1* genes (Figs. 1 and 4). However, in the sink leaf, a transient accumulation of starch was observed until day 8, prior to undergoing degradation. This original behaviour was not intuitively deduced from the transcriptional regulation of starch synthase genes and raised questions about the underlying mechanisms involved in this accumulation. In Arabidopsis, a previous study identified a small increase in starch during moderate and severe water deficits,

accompanied by an accumulation of numerous plant central metabolites (Hummel et al., 2010). The underlying mechanism responsible for these accumulations was based on a growth arrest, which could result in a reduction in the C consumption/C available ratio. This, in turn, would lead to an overall increase in starch reserves and other soluble metabolites (Ribeiro et al., 2022). Here, the growth and expansion of leaf 11 was limited by drought (Fig. 1, Fig. S4) and a multitude of amino acids, sugars and organic acids were accumulated in the leaf 11 (Fig. 3 clusters I, II). Nevertheless, a significant reduction of stomatal conductance was observed concurrently (day 8), which could potentially rebalance the ratio of C consumption to C availability for the sink leaves. It is also important to consider the contribution of source-to-sink remobilisation of sucrose to the transient accumulation of starch during drought. Young leaves have a strong sucrose uptake capacity compared to old leaves (Dethloff et al., 2017). In the source leaf, the activation of senescence and starch degradation occurred after 4–8 days of drought, and was subsequently associated with an induction of sucrose synthase and sucrose transporter genes, particularly *SUS1*, *SUS3* and *SUC2* (Figs. 2 and 4). However, there can be a notable discrepancy between the final expression levels of *SUC2* and the resulting sucrose content in phloem exudates in different plant species including rapeseed (La et al., 2019; Park et al., 2021; Xu et al., 2018). Source strength and post-translational modifications of SUC proteins appear to be the major determinants in phloem loading of sucrose (Xu et al., 2018). Interestingly, drought reinforced the source status of leaf 4, as evidenced by the higher expression of *SAG12* and the decrease of chlorophyll and protein contents, which were observed after 8–11 days of drought. However, ADP-glucose pyrophosphorylase rather than SUSY, is implicated in the biosynthesis of ADP-glucose in chloroplasts, which serves as the substrate for starch synthases (Funfgeld et al., 2022). Perhaps the remobilised sucrose could be primarily processed by neutral invertases and glycolytic enzymes to produce hexose phosphates, which would act as precursors for ADP-glucose biosynthesis (Figueroa et al., 2022). Indeed, the activity of neutral INV was relatively maintained during drought in the sink leaf compared to the activity of acid INV (Fig. 4B). The transient accumulation of starch in sink leaves during drought remains an intriguing phenomenon that should be further investigated (Fig. 7).

4.2. *Are stored citrate and malate the main substrates of TCA cycle activity in sink leaves during drought?*

Malate and citrate were identified as the organic acids of the TCA cycle, with the highest concentrations observed in WOSR leaves. In different plants, these compounds are primarily located in the leaf vacuole, where they function as C storage molecules, irrespective of the leaf sink/source status (Destailleur et al., 2021; Szecowka et al., 2013). In response to drought, leaf 11 exhibited a reduction in citrate content and a diminished accumulation of malate in comparison to the control condition (Fig. 5A). These behaviours could be attributed to both a decline in *de novo* biosynthesis and an increase in utilisation. It has been proposed that stored citrate contributes to TCA cycle activity in plants according to a day/night scheme (Le and Millar, 2022). Nevertheless, recent experiments in WOSR showed that stored citrate only contributed to Glu biosynthesis in the cytosol (Dellero et al., 2023a). Here, drought significantly reduced total CS activity in leaf 11 at day 8 and day 15 (Fig. 5B). Given that numerous *P5CS1* genes were induced in sink leaves after 8 and 15 days of drought (Fig. 6B), stored citrate was presumably used for *de novo* Pro biosynthesis in sink leaves through 2-oxoglutarate production (Fig. 7). However, the production of Glu from 2-oxoglutarate could be partially limited in sink leaves by the reduced expression of the *GLN1.1* and *GLN1.4* genes (GS/GOGAT cycle), in accordance with the reduction in leaf growth (Figs. 1 and 6, Fig. S4). Stored malate has been identified as the major contributor to mitochondrial TCA cycle activity in the light in WOSR based on the isotopic pattern of citrate, Glu and succinate (Dellero et al., 2023a, 2023b). Given that the cyclic mode of the TCA cycle can operate at an important rate in WOSR, the maintenance of malate levels could be a logical outcome of both TCA cycle and PEPc activities. In response to a short-term transition to a low CO_2 atmosphere, PEPc activity can increase (Abadie and Tcherkez, 2019). Although this low CO_2 atmospheric condition can be partially met when stomatal conductance declines, drought significantly reduced total PEPc activity in leaf 11 at day 8. Overall, the maintenance of malate levels during drought in sink leaves may be indicative of the malate/oxaloacetate shuttle's pivotal role in exporting extra-reducing power outside of chloroplasts, thereby avoiding ROS production (Igamberdiev and Bykova, 2023; Selinski and Scheibe, 2019).

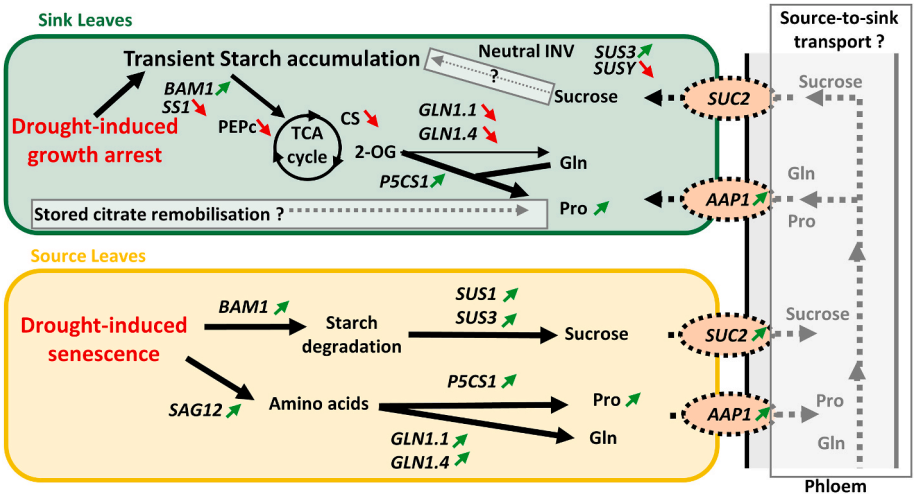

Fig. 7. Proposed model of metabolic acclimation of WOSR in response to drought: a trade-off between the senescence of source leaves and the growth arrest of sink leaves. The small green and red arrows indicate the levels of transcripts, metabolites and enzyme activities that increase or decrease during drought. Dotted arrows show assumed metabolic contributions that require further investigations to be validated. *AAP*, amino acid permease; *BAM*, beta-amylase; CS, citrate synthase; INV, invertase; *GLN*, glutamine synthetase; *P5CS*, pyrroline-5-carboxylate synthetase; PEPc, phosphoenolpyruvate carboxylase; *SAG*, senescence-associated gene; SS, starch synthase; *SUS*/SUSY, sucrose synthase; *SUC*, sucrose proton symporter; TCA cycle, tricarboxylic acid cycle. (For interpretation of the references to colour in this figure legend, the reader is referred to the Web version of this article.)

4.3. The metabolic origin of C and N into Pro during drought conditions in both sink and source leaves

The accumulation of Pro in sink and source leaves during the drought was positively correlated with the decrease in leaf RWC (Figs. 1E and 6A). This result highlighted the well-known osmoregulatory role of Pro in rapeseed leaves, which allowed for the reduction of drought-induced water losses (Boulc'h et al., 2024; Sanders and Arndt, 2012; Slama et al., 2015). However, the regulation of plant central metabolism during drought indicated that a range of pathways and mechanisms contributed to the support of Pro biosynthesis in source and sink leaves (Fig. 7). In the source leaf, drought stimulated senescence-induced protein degradation (Fig. 2). Water-soluble proteins and insoluble proteins can represent respectively 25–30% of total leaf N in WOSR (Liu et al., 2018). Conversely, NO_3^- and NH_4^+ ions are found in low concentrations in WOSR (Boulc'h et al., 2024). The level of these ions was not significantly reduced by the drought, suggesting the involvement of organic N in Pro biosynthesis (Fig. S11). Therefore, Pro arising from protein degradation was likely sufficient to meet the needs of the source leaf. Nevertheless, the active production of Pro from Glu in the source leaf during drought may have been stimulated by the induction of *P5CS1* genes (Fig. 6). To this end, amino acid catabolism may be the primary contributor to this phenomenon, as observed in Arabidopsis (Heinemann et al., 2021). It seems unlikely that starch degradation was involved in the *de novo* biosynthesis of 2-oxoglutarate (TCA cycle) to support Pro production between days 11 and 15 in the source leaf, given that starch contents were undetectable at day 11. Presumably, starch degradation in source leaves primarily fuel source-to-sink remobilisation of sucrose in the early stages of drought.

In the sink leaf, starch degradation could contribute to Pro biosynthesis during drought, given the concomitant decrease in starch content and the up-regulation of *BAM1* genes (Figs. 4 and 6). A similar role has been proposed using *bam1* Arabidopsis mutant cultivated under osmotic stress (Zanella et al., 2016). The contribution of stored citrate in Pro production could also be assumed, based on the regulation of TCA cycle enzyme activities and the decrease in citrate content during drought (Fig. 7). However, it is also possible that Pro can be directly remobilised from source to sink leaves. Leaf phloem sap is generally enriched in Pro during drought in different plant species (Albert et al., 2012; Lee et al., 2009; Stallmann et al., 2022). Among the amino acid permease transporters, *AAP1* is often expressed during abiotic stress and preferentially transports Pro (Cui et al., 2023; Ji et al., 2020; Tilsner et al., 2005; Wang et al., 2017). In this study, drought induced the up-regulation of *BnaA.C.AAP1* genes in both sink and source leaves. Consequently, *AAP1*-mediated transport of Pro from source to sink leaves during drought is a plausible scenario. In addition, the source-to-sink remobilisation of other metabolites may also contribute to Pro biosynthesis indirectly, given that phloem sap is often enriched in Gln and sucrose (Lohaus and Moellers, 2000; Tilsner et al., 2005; Xu et al., 2018). Here, the expression of two genes *BnaA.GLN1.1a* and *BnaA.GLN1.4b*, which encode major isoforms controlling Gln biosynthesis for N remobilisation (Moison et al., 2018; Orsel et al., 2014), was found to be up-regulated at day 15. These genes exhibited higher expression in source leaves of WOSR compared to sink leaves during different abiotic stresses [this work, Fig. S8; (Orsel et al., 2014)]. The extent to which Gln from remobilisation can enter into Pro production remains to be determined. Finally, protein degradation will not be considered here, as it is known that WOSR accumulates large amounts of cysteine protease inhibitors in sink leaves in response to drought (Avice and Etienne, 2014; Downing et al., 1992).

To conclude, the acclimation of WOSR to drought involved concerted metabolic regulations in sink and source leaves. Sink leaves exhibited a significant reduction in growth, resulting in a transient accumulation of starch that was likely supported by the remobilisation of carbons from different sources (photosynthesis, imported sucrose, stored citrate). Subsequently, the *BAM1*-dependent starch degradation occurred and coincided with Pro accumulation. Source leaves undergo an accelerated senescence and accumulated Pro during drought. Both mechanisms may facilitate Pro accumulation in sink leaves through source-to-sink remobilisation processes mediated by *AAP1*, *GLN1.1* and *GLN1.4* genes. The investigation of TCA cycle in sink leaves suggested the maintenance of a significant cyclic flux mode during drought. Future studies should investigate the metabolic fluxes within plant central metabolism during these acclimation events using ^{13}C-labelling strategies.

CRediT authorship contribution statement

Mathieu Aubert: Writing – original draft, Visualization, Validation, Investigation, Formal analysis, Data curation. **Vanessa Clouet:** Validation, Investigation. **Florian Guilbaud:** Validation, Investigation. **Solenne Berardocco:** Validation, Investigation. **Nathalie Marnet:** Validation, Investigation. **Alain Bouchereau:** Writing – review & editing, Supervision, Project administration, Funding acquisition, Conceptualization. **Younès Dellero:** Writing – review & editing, Writing – original draft, Visualization, Validation, Supervision, Project administration, Investigation, Funding acquisition, Data curation, Conceptualization.

Data availability

The data presented in this study are available in the article and in the Supplementary data. Raw data for metabolic analyses area available from the authors upon reasonable request.

Funding

M.A. was supported by a PhD grant from the Région Bretagne and the French Research Ministry (MESR, Ministère de l'Enseignement Supérieur et de la Recherche). This work was supported by the IB2021_TRICYCLE project funded by the Plant breeding and biology department from the National Research Institute for Agriculture, Food and Environment and by the ELECTRA project funded by the University of Rennes (Scientific challenges 2023 call).

Declaration of competing interest

The authors declare that they have no known competing financial interests or personal relationships that could have appeared to influence the work reported in this paper.

Acknowledgments

We acknowledge Patrick Leconte and Anne-Marie Denis for technical assistance during plant growth and phenotyping. We thank the Metabolic Profiling and Metabolomic Platform (P2M2, https://p2m2.hub.inrae.fr/) for providing instrument devices and training to quantify plant central metabolites. We would like to express our gratitude to the Bordeaux metabolome platform for their valuable input during the implementation of enzyme activity measurements. We gratefully acknowledge financial support from the funders.

Appendix A. Supplementary data

Supplementary data to this article can be found online at https://doi.org/10.1016/j.jplph.2024.154377.

Data availability

All the data are available in the supplementals

References

Abadie, C., Tcherkez, G., 2019. *In vivo* phosphoenolpyruvate carboxylase activity is controlled by CO2 and O2 mole fractions and represents a major flux at high photorespiration rates. New Phytol. 221 (4), 1843–1852.

Albert, B., Dellero, Y., Leport, L., Aubert, M., Bouchereau, A., Le Cahérec, F., 2024. Low nitrogen input mitigates quantitative but not qualitative reconfiguration of leaf primary metabolism in Brassica napus L. Subjected to drought and rehydration. Plants.

Albert, B., Le Cahérec, F., Niogret, M.F., Faes, P., Avice, J.C., Leport, L., Bouchereau, A., 2012. Nitrogen availability impacts oilseed rape (Brassica napus L.) plant water status and proline production efficiency under water-limited conditions. Planta 236 (2), 659–676.

Avice, J.C., Etienne, P., 2014. Leaf senescence and nitrogen remobilization efficiency in oilseed rape (Brassica napus L.). J. Exp. Bot. 65 (14), 3813–3824.

Barros, J.A.S., Siqueira, J.A.B., Cavalcanti, J.H.F., Araujo, W.L., Avin-Wittenberg, T., 2020. Multifaceted roles of plant autophagy in lipid and energy metabolism. Trends Plant Sci. 25 (11), 1141–1153.

Batool, M., El-Badri, A.M., Hassan, M.U., Haiyun, Y., Chunyun, W., Zhenkun, Y., Jie, K., Wang, B., Zhou, G., 2022. Drought stress in Brassica napus: effects, tolerance mechanisms, and management strategies. J. Plant Growth Regul. 42 (1), 21–45.

Benard, C., Gibon, Y., 2016. Measurement of enzyme activities and optimization of continuous and discontinuous assays. Curr. Protoc. Plant Biol. 1 (2), 247–262.

Berrocoso, J.D., Rojas, O.J., Liu, Y., Shoulders, J., González-Vega, J.C., Stein, H.H., 2015. Energy concentration and amino acid digestibility in high-protein canola meal, conventional canola meal, and soybean meal fed to growing pigs. J. Anim. Sci. 93 (5), 2208–2217.

Biais, B., Benard, C., Beauvoit, B., Colombie, S., Prodhomme, D., Menard, G., Bernillon, S., Gehl, B., Gautier, H., Ballias, P., Mazat, J.P., Sweetlove, L., Genard, M., Gibon, Y., 2014. Remarkable reproducibility of enzyme activity profiles in tomato fruits grown under contrasting environments provides a roadmap for studies of fruit metabolism. Plant Physiol. 164 (3), 1204–1221.

Bianchetti, G., Baron, C., Carrillo, A., Berardocco, S., Marnet, N., Wagner, M.H., Demilly, D., Ducournau, S., Manzanares-Dauleux, M.J., Cahérec, F.L., Buitink, J., Nesi, N., 2021. Dataset for the metabolic and physiological characterization of seeds from oilseed rape (Brassica napus L.) plants grown under single or combined effects of drought and clubroot pathogen Plasmodiophora brassicae. Data Brief 37, 107247.

Bouchet, A.-S., Laperche, A., Bissuel-Belaygue, C., Snowdon, R., Nesi, N., Stahl, A., 2016. Nitrogen use efficiency in rapeseed. A review. Agron. Sustain. Dev. 36 (2).

Boulc'h, P.N., Clouet, V., Niogret, M.F., Avice, J.C., Musse, M., Leport, L., 2024. Leaf drought adaptive response in winter oilseed rape is altered at the onset of senescence: a study combining NMR relaxometry, multi-omics and microscopy. Physiol. Plantarum 176 (4), e14454.

Chrobok, D., Law, S.R., Brouwer, B., Linden, P., Ziolkowska, A., Liebsch, D., Narsai, R., Szal, B., Moritz, T., Rouhier, N., Whelan, J., Gardestrom, P., Keech, O., 2016. Dissecting the metabolic role of mitochondria during developmental leaf senescence. Plant Physiol. 172 (4), 2132–2153.

Cui, R., Feng, Y., Yao, J., Shi, L., Wang, S., Xu, F., 2023. The transcription factor BnaA9. WRKY47 coordinates leaf senescence and nitrogen remobilization in Brassica napus. J. Exp. Bot. 74 (18), 5606–5619.

D'Oria, A., Jing, L., Arkoun, M., Pluchon, S., Pateyron, S., Trouverie, J., Etienne, P., Diquelou, S., Ourry, A., 2022. Transcriptomic, metabolomic and ionomic analyses reveal early modulation of leaf mineral content in Brassica napus under mild or severe drought. Int. J. Mol. Sci. 23 (2).

da Fonseca-Pereira, P., Souza, P.V.L., Fernie, A.R., Timm, S., Daloso, D.M., Araujo, W.L., 2021. Thioredoxin-mediated regulation of (photo)respiration and central metabolism. J. Exp. Bot. 72 (17), 5987–6002.

Dellero, Y., 2020. Manipulating amino acid metabolism to improve crop nitrogen use efficiency for a sustainable agriculture. Front. Plant Sci. 11, 1857.

Dellero, Y., Berardocco, S., Berges, C., Filangi, O., Bouchereau, A., 2023a. Validation of carbon isotopologue distribution measurements by GC-MS and application to 13C-metabolic flux analysis of the tricarboxylic acid cycle in Brassica napus leaves. Front. Plant Sci. 13, 22.

Dellero, Y., Berardocco, S., Bouchereau, A., 2023b. U-(13)C-glucose incorporation into source leaves of Brassica napus highlights light-dependent regulations of metabolic fluxes within central carbon metabolism. J. Plant Physiol. 292, 154162.

Dellero, Y., Clouet, V., Marnet, N., Pellizzaro, A., Dechaumet, S., Niogret, M.F., Bouchereau, A., 2020a. Leaf status and environmental signals jointly regulate proline metabolism in winter oilseed rape. J. Exp. Bot. 71 (6), 2098–2111.

Dellero, Y., Heuillet, M., Marnet, N., Bellvert, F., Millard, P., Bouchereau, A., 2020b. Sink/source balance of leaves influences amino acid pools and their associated metabolic fluxes in winter oilseed rape (Brassica napus L.). Metabolites 10 (4), 16.

Dellero, Y., Jossier, M., Bouchereau, A., Hodges, M., Leport, L., 2021a. Leaf phenological stages of winter oilseed rape (Brassica napus L.) have conserved photosynthetic efficiencies but contrasted intrinsic water use efficiencies at high light intensities. Front. Plant Sci. 12.

Dellero, Y., Lamothe-Sibold, M., Jossier, M., Hodges, M., 2015. Arabidopsis thaliana ggt1 photorespiratory mutants maintain leaf carbon/nitrogen balance by reducing RuBisCO content and plant growth. Plant J. 83 (6), 1005–1018.

Dellero, Y., Mauve, C., Jossier, M., Hodges, M., 2021b. The impact of photorespiratory glycolate oxidase activity on Arabidopsis thaliana leaf soluble amino acid pool sizes during acclimation to low atmospheric CO2 concentrations. Metabolites 11 (8), 501.

Destailleur, A., Poucet, T., Cabasson, C., Alonso, A.P., Cocuron, J.C., Larbat, R., Vercambre, G., Colombie, S., Petriacq, P., Andrieu, M.H., Beauvoit, B., Gibon, Y., Dieuaide-Noubhani, M., 2021. The evolution of leaf function during development is reflected in profound changes in the metabolic composition of the vacuole. Metabolites 11 (12).

Dethloff, F., Orf, I., Kopka, J., 2017. Rapid *in situ* (13)C tracing of sucrose utilization in Arabidopsis sink and source leaves. Plant Method. 13, 87.

Dominguez, F., Cejudo, F.J., 2021. Chloroplast dismantling in leaf senescence. J. Exp. Bot. 72 (16), 5905–5918.

Downing, W., Mauxion, F., Fauvarque, M., Reviron, M., De Vienne, D., Vartanian, N., Giraudat, J., 1992. A Brassica napus transcript encoding a protein related to the Kunitz protease inhibitor family accumulates upon water stress in leaves, not in seeds. Plant J. 2 (5), 685–693.

Eigentler, A., Draxl, A., Gnaiger, E., 2020. Laboratory Protocol: citrate synthase a mitochondrial marker enzyme. Mitochondr. Physiol. Netw. 17 (4), 13.

Elferjani, R., Soolanayakanahally, R., 2018. Canola responses to drought, heat, and combined stress: shared and specific effects on carbon assimilation, seed yield, and oil composition. Front. Plant Sci. 9, 1224.

Fabregas, N., Fernie, A.R., 2019. The metabolic response to drought. J. Exp. Bot. 70 (4), 1077–1085.

Feller, U., Vaseva, I.I., 2014. Extreme climatic events: impacts of drought and high temperature on physiological processes in agronomically important plants. Front. Environ. Sci. 2.

Figueroa, C.M., Asencion Diez, M.D., Ballicora, M.A., Iglesias, A.A., 2022. Structure, function, and evolution of plant ADP-glucose pyrophosphorylase. Plant Mol. Biol. 108 (4–5), 307–323.

Fu, X., Gregory, L.M., Weise, S.E., Walker, B.J., 2022. Integrated flux and pool size analysis in plant central metabolism reveals unique roles of glycine and serine during photorespiration. Nat. Plants 9, 12.

Funfgeld, M., Wang, W., Ishihara, H., Arrivault, S., Feil, R., Smith, A.M., Stitt, M., Lunn, J.E., Niittyla, T., 2022. Sucrose synthases are not involved in starch synthesis in Arabidopsis leaves. Nat. Plants 8 (5), 574–582.

Gibon, Y., Blaesing, O.E., Hannemann, J., Carillo, P., Hohne, M., Hendriks, J.H., Palacios, N., Cross, J., Selbig, J., Stitt, M., 2004. A Robot-based platform to measure multiple enzyme activities in Arabidopsis using a set of cycling assays: comparison of changes of enzyme activities and transcript levels during diurnal cycles and in prolonged darkness. Plant Cell 16 (12), 3304–3325.

Gomez, L., Bancel, D., Rubio, E., Vercambre, G., 2007. The microplate reader: an efficient tool for the separate enzymatic analysis of sugars in plant tissues—validation of a micro-method. J. Sci. Food Agric. 87 (10), 1893–1905.

Harkness, C., Semenov, M.A., Areal, F., Senapati, N., Trnka, M., Balek, J., Bishop, J., 2020. Adverse weather conditions for UK wheat production under climate change. Agric. For. Meteorol. 282–283, 107862.

Have, M., Marmagne, A., Chardon, F., Masclaux-Daubresse, C., 2017. Nitrogen remobilization during leaf senescence: lessons from Arabidopsis to crops. J. Exp. Bot. 68 (10), 2513–2529.

Heinemann, B., Kunzler, P., Eubel, H., Braun, H.P., Hildebrandt, T.M., 2021. Estimating the number of protein molecules in a plant cell: protein and amino acid homeostasis during drought. Plant Physiol. 185 (2), 385–404.

Hellemans, J., Mortier, G., De Paepe, A., Speleman, F., Vandesompele, J., 2007. qBase relative quantification framework and software for management and automated analysis of real-time quantitative PCR data. Genome Biol. 8 (2), R19.

Hummel, I., Pantin, F., Sulpice, R., Piques, M., Rolland, G., Dauzat, M., Christophe, A., Pervent, M., Bouteille, M., Stitt, M., Gibon, Y., Muller, B., 2010. Arabidopsis plants acclimate to water deficit at low cost through changes of carbon usage: an integrated perspective using growth, metabolite, enzyme, and gene expression analysis. Plant Physiol. 154 (1), 357–372.

Igamberdiev, A.U., Bykova, N.V., 2023. Mitochondria in photosynthetic cells: coordinating redox control and energy balance. Plant Physiol. 191 (4), 2104–2119.

Ji, Y., Huang, W., Wu, B., Fang, Z., Wang, X., 2020. The amino acid transporter OsAAP1 mediates growth and grain yield by regulating neutral amino acids uptake and reallocation in Oryza sativa. J. Exp. Bot.

Kuromori, T., Seo, M., Shinozaki, K., 2018. ABA transport and plant water stress responses. Trends Plant Sci. 23 (6), 513–522.

La, V.H., Lee, B.-R., Islam, M.T., Park, S.-H., Lee, H., Bae, D.-W., Kim, T.-H., 2019. Antagonistic shifting from abscisic acid- to salicylic acid-mediated sucrose accumulation contributes to drought tolerance in Brassica napus. Environ. Exp. Bot. 162, 38–47.

Le, X.H., Millar, A.H., 2022. The diversity of substrates for plant respiration and how to optimize their use. Plant Physiol.

Lee, B.R., Jin, Y.L., Avice, J.C., Cliquet, J.B., Ourry, A., Kim, T.H., 2009. Increased proline loading to phloem and its effects on nitrogen uptake and assimilation in water-stressed white clover (Trifolium repens). New Phytol. 182 (3), 654–663.

Liu, T., Ren, T., White, P.J., Cong, R., Lu, J., 2018. Storage nitrogen co-ordinates leaf expansion and photosynthetic capacity in winter oilseed rape. J. Exp. Bot. 69 (12), 2995–3007.

Lohaus, G., Moellers, C., 2000. Phloem transport of amino acids in two Brassica napus L. genotypes and one B. carinata genotype in relation to their seed protein content. Planta 211 (6), 833–840.

Ma, Q., Turner, D.W., Levy, D., Cowling, W.A., 2004. Solute accumulation and osmotic adjustment in leaves of Brassica oilseeds in response to soil water deficit. Aust. J. Agric. Res. 55 (9), 939.

Malagoli, P., Laine, P., Rossato, L., Ourry, A., 2005. Dynamics of nitrogen uptake and mobilization in field-grown winter oilseed rape (Brassica napus) from stem extension to harvest: I. Global N flows between vegetative and reproductive tissues in relation to leaf fall and their residual N. Ann. Bot. 95 (5), 853–861.

Moison, M., Marmagne, A., Dinant, S., Soulay, F., Azzopardi, M., Lothier, J., Citerne, S., Morin, H., Legay, N., Chardon, F., Avice, J.C., Reisdorf-Cren, M., Masclaux-Daubresse, C., 2018. Three cytosolic glutamine synthetase isoforms localized in

different-order veins act together for N remobilization and seed filling in Arabidopsis. J. Exp. Bot. 69 (18), 4379–4393.
Nakamura, S., Izumi, M., 2018. Regulation of chlorophagy during photoinhibition and senescence: lessons from mitophagy. Plant Cell Physiol. 59 (6), 1135–1143.
Nunes-Nesi, A., Araujo, W.L., Obata, T., Fernie, A.R., 2013. Regulation of the mitochondrial tricarboxylic acid cycle. Curr. Opin. Plant Biol. 16 (3), 335–343.
Orsel, M., Moison, M., Clouet, V., Thomas, J., Leprince, F., Canoy, A.S., Just, J., Chalhoub, B., Masclaux-Daubresse, C., 2014. Sixteen cytosolic glutamine synthetase genes identified in the Brassica napus L. genome are differentially regulated depending on nitrogen regimes and leaf senescence. J. Exp. Bot. 65 (14), 3927–3947.
Park, S.H., Lee, B.R., La, V.H., Mamun, M.A., Bae, D.W., Kim, T.H., 2021. Drought intensity-responsive salicylic acid and abscisic acid crosstalk with the sugar signaling and metabolic pathway in Brassica napus. Plants 10 (3).
Pires, M.V., Pereira Junior, A.A., Medeiros, D.B., Daloso, D.M., Pham, P.A., Barros, K.A., Engqvist, M.K., Florian, A., Krahnert, I., Maurino, V.G., Araujo, W.L., Fernie, A.R., 2016. The influence of alternative pathways of respiration that utilize branched-chain amino acids following water shortage in Arabidopsis. Plant Cell Environ. 39 (6), 1304–1319.
Pörtner, H.-O., Roberts, D.C., Tignor, M., Poloczanska, E.S., Mintenbeck, K., Alegria, A., Craig, M., Langsdorf, S., Loschke, S., Moller, V., Okem, A., Rama, B., 2022. Climate Change 2022: Impacts, Adaptation, and Vulnerability, 3056. Cambridge University Press, C., United Kingdom and New York, NY, USA.
Renault, H., Roussel, V., El Amrani, A., Arzel, M., Renault, D., Bouchereau, A., Deleu, C., 2010. The Arabidopsis pop2-1 mutant reveals the involvement of GABA transaminase in salt stress tolerance. BMC Plant Biol. 10, 20.
Ribeiro, C., Stitt, M., Hotta, C.T., 2022. How stress affects your budget-stress impacts on starch metabolism. Front. Plant Sci. 13, 774060.
Rolland, S., Lucile, R., Leprince, F., Alix, E., Carrillo, A., Guichard, S., Moulin, B., Alina, T., Tardy, C., Le Cahérec, F., Nesi, N., Laperche, A., 2018. Development and Validation of Near-Infrared Spectroscopy Models for Predicting Nitrogen and Carbon Contents in Rapeseed Tissues (Brassica Napus), Brassica 2018. Saint-Malo, France.
Rosado-Souza, L., Yokoyama, R., Sonnewald, U., Fernie, A.R., 2023. Understanding source-sink interactions: progress in model plants and translational research to crops. Mol. Plant 16 (1), 96–121.
Rousseau-Gueutin, M., Belser, C., Da Silva, C., Richard, G., Istace, B., Cruaud, C., Falentin, C., Boideau, F., Boutte, J., Delourme, R., Deniot, G., Engelen, S., de Carvalho, J.F., Lemainque, A., Maillet, L., Morice, J., Wincker, P., Denoeud, F., Chevre, A.M., Aury, J.M., 2020. Long-read assembly of the Brassica napus reference genome Darmor-bzh. GigaScience 9 (12).
RStudio Team, 2022. R: A Lang. Environ. Stat. Comput.
Sanders, G.J., Arndt, S.K., 2012. Osmotic adjustment under drought conditions. Plant Respons. Drou. Str. 199–229.
Sehgal, A., Sita, K., Siddique, K.H.M., Kumar, R., Bhogireddy, S., Varshney, R.K., HanumanthaRao, B., Nair, R.M., Prasad, P.V.V., Nayyar, H., 2018. Drought or/and heat-stress effects on seed filling in food crops: impacts on functional biochemistry, seed yields, and nutritional quality. Front. Plant Sci. 9, 1705.
Selinski, J., Scheibe, R., 2019. Malate valves: old shuttles with new perspectives. Plant Biol. 21 (Suppl. 1), 21–30.
Slama, I., Abdelly, C., Bouchereau, A., Flowers, T., Savoure, A., 2015. Diversity, distribution and roles of osmoprotective compounds accumulated in halophytes under abiotic stress. Ann. Bot. 115 (3), 433–447.
Sonnewald, U., Fernie, A.R., 2018. Next-generation strategies for understanding and influencing source-sink relations in crop plants. Curr. Opin. Plant Biol. 43, 63–70.
Stallmann, J., Pons, C.A.A., Schweiger, R., Muller, C., 2022. Time point- and plant part-specific changes in phloem exudate metabolites of leaves and ears of wheat in response to drought and effects on aphids. PLoS One 17 (1), e0262671.
Stein, O., Granot, D., 2019. An overview of sucrose synthases in plants. Front. Plant Sci. 10, 95.
Szecowka, M., Heise, R., Tohge, T., Nunes-Nesi, A., Vosloh, D., Huege, J., Feil, R., Lunn, J., Nikoloski, Z., Stitt, M., Fernie, A.R., Arrivault, S., 2013. Metabolic fluxes in an illuminated Arabidopsis rosette. Plant Cell 25 (2), 694–714.
Tardieu, F., Simonneau, T., Muller, B., 2018. The physiological basis of drought tolerance in crop plants: a scenario-dependent probabilistic approach. Annu. Rev. Plant Biol. 69, 733–759.
Tegeder, M., Hammes, U.Z., 2018. The way out and in: phloem loading and unloading of amino acids. Curr. Opin. Plant Biol. 43, 16–21.
Thalmann, M., Santelia, D., 2017. Starch as a determinant of plant fitness under abiotic stress. New Phytol. 214 (3), 943–951.
Tilsner, J., Kassner, N., Struck, C., Lohaus, G., 2005. Amino acid contents and transport in oilseed rape (Brassica napus L.) under different nitrogen conditions. Planta 221 (3), 328–338.
Turner, N.C., Furbank, R.T., Berger, J.D., Gremigni, P., Abbo, S., Leport, L., 2009. Seed size is associated with sucrose synthase activity in developing cotyledons of chickpea. Crop Sci. 49 (2), 621–627.
Urban, M.O., Vasek, J., Klima, M., Krtkova, J., Kosova, K., Prasil, I.T., Vitamvas, P., 2017. Proteomic and physiological approach reveals drought-induced changes in rapeseeds: water-saver and water-spender strategy. J. Proteonomics 152, 188–205.
Vazquez-Carrasquer, V., Laperche, A., Bissuel-Belaygue, C., Chelle, M., Richard-Molard, C., 2021. Nitrogen uptake efficiency, mediated by fine root growth, early determines temporal and genotypic variations in nitrogen use efficiency of winter oilseed rape. Front. Plant Sci. 12, 641459.
Verslues, P.E., Bailey-Serres, J., Brodersen, C., Buckley, T.N., Conti, L., Christmann, A., Dinneny, J.R., Grill, E., Hayes, S., Heckman, R.W., Hsu, P.K., Juenger, T.E., Mas, P., Munnik, T., Nelissen, H., Sack, L., Schroeder, J.I., Testerink, C., Tyerman, S.D., Umezawa, T., Wigge, P.A., 2023. Burning questions for a warming and changing world: 15 unknowns in plant abiotic stress. Plant Cell 35 (1), 67–108.
Wang, C., Linderholm, H.W., Song, Y., Wang, F., Liu, Y., Tian, J., Xu, J., Song, Y., Ren, G., 2020. Impacts of drought on maize and soybean production in northeast China during the past five decades. Int. J. Environ. Res. Publ. Health 17 (7).
Wang, T., Chen, Y., Zhang, M., Chen, J., Liu, J., Han, H., Hua, X., 2017. Arabidopsis AMINO ACID PERMEASE1 contributes to salt stress-induced proline uptake from exogenous sources. Front. Plant Sci. 8, 2182.
Wang, W., Tai, F., Chen, S., 2008. Optimizing protein extraction from plant tissues for enhanced proteomics analysis. J. Separ. Sci. 31 (11), 2032–2039.
Wei, R., Wang, J., Su, M., Jia, E., Chen, S., Chen, T., Ni, Y., 2018. Missing value imputation approach for mass spectrometry-based metabolomics data. Sci. Rep. 8 (1), 663.
Xiong, J.L., Ma, N., 2022. Transcriptomic and metabolomic analyses reveal that fullerol improves drought tolerance in Brassica napus L. Int. J. Mol. Sci. 23 (23).
Xu, Q., Chen, S., Yunjuan, R., Chen, S., Liesche, J., 2018. Regulation of sucrose transporters and phloem loading in response to environmental cues. Plant Physiol. 176 (1), 930–945.
Zandalinas, S.I., Fritschi, F.B., Mittler, R., 2021. Global warming, climate change, and environmental pollution: recipe for a multifactorial stress combination disaster. Trends Plant Sci. 26 (6), 588–599.
Zanella, M., Borghi, G.L., Pirone, C., Thalmann, M., Pazmino, D., Costa, A., Santelia, D., Trost, P., Sparla, F., 2016. beta-amylase 1 (BAM1) degrades transitory starch to sustain proline biosynthesis during drought stress. J. Exp. Bot. 67 (6), 1819–1826.